

Anomalous diamagnetism of electrider electrons in transition metal silicidesM. Hiraishi¹, K. M. Kojima^{1,2}, H. Okabe¹, A. Koda^{1,2}, R. Kadono^{1,2}, J. Wu³, Y. Lu³, and H. Hosono³¹*Muon Science Laboratory and Condensed Matter Research Center, Institute of Materials Structure Science, High Energy Accelerator Research Organization (KEK-IMSS), Tsukuba, Ibaraki 305-0801, Japan*²*Department of Materials Structure Science, The Graduate University for Advanced Studies (Sokendai), Tsukuba, Ibaraki 305-0801, Japan*³*Materials Research Center for Element Strategy, Tokyo Institute of Technology (MCES), Yokohama, Kanagawa 226-8503, Japan* (Received 19 March 2021; revised 19 May 2021; accepted 21 May 2021; published 1 June 2021)

Intermetallic silicide compounds, LaScSi and Y₅Si₃, known for being hydrogen (H) storage materials, are drawing attention as candidates for electrides in which anions are substituted by unbound electrons. It is inferred from a muon spin rotation experiment that the local field at the muon site (which is the same site as that for H) in these compounds exhibits a large negative shift under an external magnetic field, which is mostly independent of temperature. Such anomalous diamagnetism signals a unique property of electrider electrons associated with transition metals. Moreover, the diamagnetic shift decreases with increasing H content, suggesting that the electrider electrons existing coherently in the hollow interstitial positions are adsorbed by H to form hydride ions (H⁻).

DOI: [10.1103/PhysRevB.103.L241101](https://doi.org/10.1103/PhysRevB.103.L241101)**I. INTRODUCTION**

Electrides are a class of materials in which excess electrons are accommodated in voids as anions without atomic nuclei [1,2]. They have been drawing much attention because of their high electron mobility, low work function, and high affinity for hydrogen. The recent demonstration of oxygen-depleted mayenite ([Ca₂₄Al₂₈O₆₄]⁴⁺4e⁻, abbreviated as C12A7 : e⁻) as the first air-stable solid electrider [3–5] has started extensive research on solid electrides. This has resulted in a breakthrough in ammonia synthesis due to the very high catalytic efficiency of ruthenium (Ru) dispersed on C12A7 : e⁻ [6,7], thus leading to various applications in related fields [8–12]. A search for candidate solid electrider compounds has also been triggered. Intermetallic silicides, which include LaScSi and Y₅Si₃, have been proposed as a new subclass of electrides [13,14]. These compounds are stable under atmospheric as well as moist conditions and have received growing interest because they can also serve as highly efficient catalysts for ammonia synthesis when dispersed with Ru.

LaScSi (space group *I4/mmm*) has layered networks of La₄ tetrahedral voids (V) and La₂Sc₄ octahedral voids (V') interlaced with Si layers [see Fig. 1(a)]. X-ray diffraction (XRD) and thermal desorption spectroscopy have shown that up to 1.5 hydrogen atoms can be stored in the V and V' sites per formula unit [13,15]. First-principles density functional theory (DFT) calculations have shown that the electrons that contribute to the density of states near the Fermi energy [*N*(*E*_F)] are localized at the center of the V and V' sites, depending on the H concentration. Because the electrider electrons in pristine LaScSi are predicted to be mostly localized at the V sites, a stepwise hydrogenation process has been proposed. In this process, H first preferentially occupies the V site to form LaScSiHV_{0.5} and then the V' site to form LaScSiH_{1.5} (tiered electron anions) [13].

Y₅Si₃ belongs to the Mn₅Si₃-type structure [space group *P6₃/mcm*; see Fig. 1(b)] and has been studied mainly as a hydrogen storage alloy [16]. The hydride Y₅Si₃H_x has been reported to accommodate H in a position coordinated by six Y atoms (*2b* site) that comprises a one-dimensional hollow channel of approximately 0.4 nm diameter running along the *c* axis. DFT calculations have indicated that a band originating from the 1s orbital of H exists at approximately 5 eV below *E*_F in Y₅Si₃H, whereas another band strongly hybridized with the 4*d* orbital of Y exists near *E*_F in pristine Y₅Si₃ [14]. The latter is presumed to originate from electrons localized at the *2b* site (electrider electrons) and contributes to the emergence of functionalities such as catalytic activity.

In C12A7 : e⁻, hydride ions are localized at the center of the cage where electrider electrons reside upon H intake [3,17]. Because of the differences in the local structure of the electrider electrons and their band characteristics between LaScSi/Y₅Si₃ and C12A7 : e⁻ (anionic electron bands strongly overlap with other atomic orbitals in the former [13,14] and the bands are virtually isolated in the latter [4]), it is important to understand the local electronic state associated with H occupancy. This state plays an important role in catalytic activity [6,7].

In this regard, it is worth mentioning that a peculiar diamagnetism has been reported in a muon spin rotation (*μ*SR) study of Y₂C [18], which is also known to be a two-dimensional electrider with H-storage capability [19–21]. Because muons acting as pseudo-H occupy the H site, which is situated in the center of the electrider electrons spread over two dimensions, it has been argued that the diamagnetism probed by muons is characteristic to the band structure of electrides that exhibit strong hybridization with Y 4*d* orbitals. Theoretical prediction of ferromagnetic instability (Stoner ferromagnetism) and inelastic neutron scattering measurement in

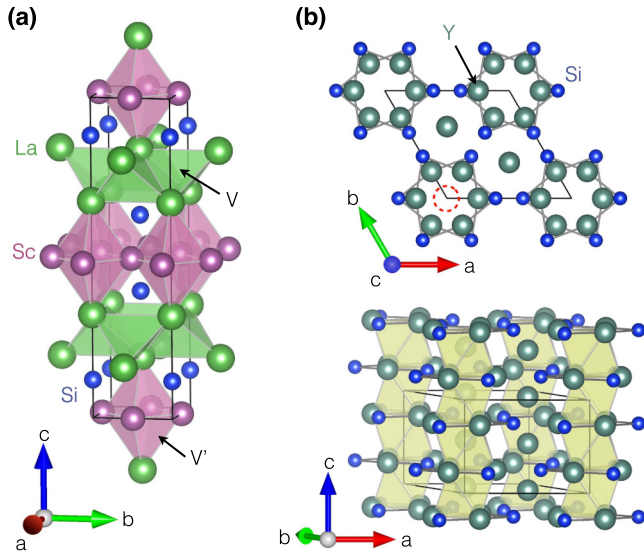


FIG. 1. Crystal structures of (a) LaScSi and (b) Y_5Si_3 . The red dashed circle in the upper part of (b) indicates a one-dimensional channel (hole) running along the c axis.

Y_2C suggest a possible link between the electrone electrons and Y $4d$ bands [20,22].

The implanted muon can be regarded as a light isotope of H (approximately $1/9m_H$, where m_H is the mass of hydrogen), which provides a unique tool for experimentally simulating interstitial H in the dilute limit. This allows spectroscopic information on the electronic structure to be obtained via μ SR. In particular, μ SR can provide information on the local valency of muons as pseudo-H (corresponding to H^\pm , H^0), which is not readily accessible by other conventional techniques. In contrast to the large difference in the mass between a muon and a proton, the difference between the reduced mass of the bound electrons is only approximately 0.4%. Thus, the local electronic structure associated with muons is almost identical to that of protons in the host matter. As the term “muonium” refers exclusively to the neutral bound state of μ^+ and e^- (i.e., to the *structure*), it would be convenient to introduce the term “muogen” (abbreviated as Mu) to describe the *properties* of muons as an element ($^{0.1126}\text{Mu}$) [23,24].

Here, we report on the microscopic properties of H and electrone electrons probed by μ SR in LaScSi and its hydrides and in Y_5Si_3 . In LaScSi and its hydrides/deuterides, the Mu occupancy of V/V' sites as pseudo-H was determined through a detailed analysis of the μ SR spectra under zero and longitudinal fields. The results were confirmed to be consistent with those inferred from DFT calculations for H at the V and V' sites in the dilute limit. The interplay between H and the electrone electrons in these compounds was investigated through the μ SR frequency shift under a magnetic field, which is proportional to the local susceptibility at the Mu site. An anomalously large negative shift was observed in pristine compounds irrespective of temperature, for which we argue a couple of possible mechanisms. The shift decreased monotonously with increasing H content, suggesting that the electrone electrons existed in a state delocalized over multiple

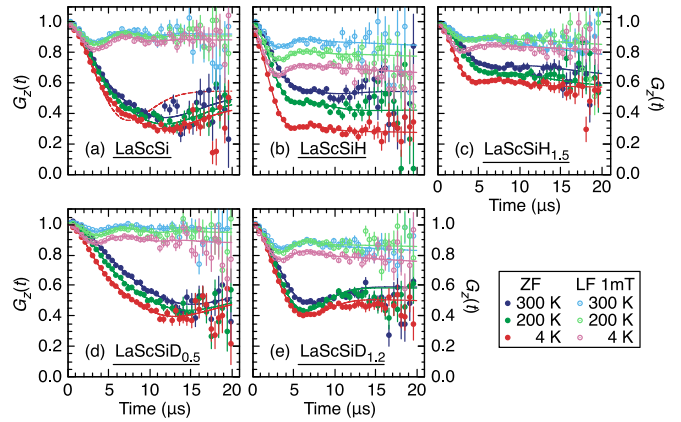


FIG. 2. μ SR time spectra under zero (ZF, closed symbol) and longitudinal (LF=1 mT, open symbol) fields observed in $LaScSiH_x$ with (a) $x = 0$, (b) $x = 1$, and (c) $x = 1.5$, and in $LaScSiD_x$ with (d) $x = 0.5$ and (e) $x = 1.2$. The solid and dashed curves in (a) are the results of curve fits using Eq. (1) with $n = 1$ and $n = 2$, respectively.

H sites and that they were localized by H to form hydride ions in the voids.

II. EXPERIMENTAL METHODS AND DFT CALCULATIONS

The polycrystalline samples of LaScSi and Y_5Si_3 used in the μ SR experiment were synthesized using the arc-melting method. The details of the sample synthesis can be found in the literature [13,14]. For LaScSi, hydrogenated and deuterated samples were prepared to investigate the mutual influence between the Mu (as pseudo-H) and electrone electrons. The four samples comprise two samples of $LaScSiH_x$ ($x = 0.9$ – 1.2 and $x \sim 1.5$, which are denoted as $x = 1$ and $x = 1.5$, respectively) and two samples of $LaScSiD_x$ ($x = 0.4$ – 0.5 and $x = 1.2$ – 1.5 , which are denoted as $x = 0.5$ and $x = 1.2$, respectively). We note that there was some uncertainty in the D content of the deuterated sample because the D content was determined empirically by comparing the results of the D content analysis with those obtained earlier for $LaScSiH_x$ (without the standard reference for D). Additional details for experiments and DFT calculations are provided in the Supplemental Material [25].

III. RESULTS

A. Mu sites: $LaScSiH_x$

Figure 2(a) shows the μ SR time spectra observed in LaScSi under zero external field (ZF) and a longitudinal field (LF) of 1 mT. The spectra are normalized by the initial asymmetry [$A(0) = A_0$] observed at ambient temperature. The ZF- μ SR spectrum exhibits a slow Gaussian depolarization due to the random local fields from the nuclear magnetic moments. A_0 is largely independent of temperature. These features indicate that most of the Mu is in a diamagnetic state (Mu^+ or Mu^-). As some of the incident muons are stopped at the backing material (silver), which has negligible depolarization, the time spectra are analyzed by using the following

TABLE I. Linewidth Δ_i in LaScSiH/D_x deduced from ZF/LF- μ SR measurements at 4 K. The simulated values for the V/V' sites in LaScSi correspond to the relaxed lattice structure obtained from the DFT calculations in the $4 \times 4 \times 1$ superlattice (192 atoms) with one hydrogen at the center of the V/V' site, whereas the others are based on structural parameters obtained by XRD [13].

		LaScSi	LaScSiH	LaScSiH _{1.5}	LaScSiD _{0.5}	LaScSiD _{1.2}
Experiment	Δ_1 (μs^{-1})	0.1468(33)	0.183(7)	0.174(9)	0.135(4)	0.286(1)
	Δ_2 (μs^{-1})	0.347(6)	0.415(4)	0.431(4)	0.348(9)	
Simulation	V center (μs^{-1})	0.1465	0.191	0.194	0.138	0.144
	V' center (μs^{-1})	0.313	0.342	0.345	0.338	0.340

function:

$$A(t) = A_0 G_z(t) = \sum_{i=1}^n A_i G_{\text{KT}}(\Delta_i, B_{\text{ext}}, \nu_i, t) + A_c, \quad (1)$$

which is approximated as

$$A(t) \simeq \sum_{i=1}^n A_i \left[\frac{1}{3} e^{-\nu_i t} + \frac{2}{3} (1 - \Delta_i^2 t^2) e^{-\Delta_i^2 t^2 / 2} \right] + A_c,$$

for the case of $\nu_i \ll \Delta_i$ and ZF ($B_{\text{ext}} = 0$). A_i is the initial asymmetry of the Mu occupying the i th site described by the Gaussian Kubo-Toyabe function, $G_{\text{KT}}(\Delta_i, B_{\text{ext}}, \nu_i, t)$, where Δ_i denotes the linewidth determined by the rms of the corresponding local field distribution (see Supplemental Material [25]), ν_i is the fluctuation rate of Δ_i , and B_{ext} is the external LF [26]. The constant term A_c consists of two contributions: one from the Mu stopped in the backing and another from the Mu that is present in the sample but exhibits no depolarization (see below).

In Fig. 2(a), the results of the least-squares fits of the ZF- μ SR spectra using Eq. (1) are shown for $n = 1$ (red dashed curves) and 2 (solid curves). The latter shows a significantly better agreement with the experimental results. This indicates that the Mu probes different magnetic field distributions at two crystallographically inequivalent sites in LaScSi. The parameter values deduced from the curve fit at the lowest temperature (4 K) are $\Delta_1 = 0.1468(33) \mu\text{s}^{-1}$ and $\Delta_2 = 0.347(6) \mu\text{s}^{-1}$. The calculated Δ values at the V and V' sites using Eq. (S1) in the Supplemental Material [25] and the lattice structure obtained from the DFT calculation [in which structural relaxation was allowed for one H in a $4 \times 4 \times 1$ supercell (192 atoms) to mimic the isolated Mu] are 0.1465 and 0.313 μs^{-1} , which are in reasonable agreement with Δ_1 and Δ_2 , respectively (see Table I). Thus, we attribute A_1 (A_2) to the signals from the Mu at the V (V') sites.

As shown in Figs. 2(b)–2(e), the depolarization rates ($\propto \Delta_i$) in LaScSiH_x and LaScSiD_x are enhanced with increasing H/D content. This enhancement is explained by the preferential occupancy of the V' sites (where the Mu exhibits a greater depolarization rate) when the V sites are fully occupied by H/D. Moreover, A_c exhibits an increase with x , as well as temperature (see Supplemental Material [25], Fig. S1.) Although the increase in Δ_i can be qualitatively attributed to the additional contribution from the nuclear magnetic moments of the nearby H, understanding the latter behavior is not trivial. As no interstitial sites are free of local magnetic fields from ^{139}La and ^{45}Sc nuclei, which have 100% natural abundance, the increase in the undamped component ($\Delta \sim 0$) suggests

that a part of the implanted Mu is subject to fast spin dynamics of unknown origin. It should be noted that a similar behavior has been reported for the hydrogen storage material NaAlH₄ [27]. An increase in A_c above approximately 100 K is observed for all the studied compositions and the increase is the most prominent in LaScSiH. Elucidation of the origin of these behaviors is an open issue to be addressed in the future.

With the exception of LaScSiD_{1.2}, the curve-fit analysis requires two components ($n = 2$) in Eq. (1), suggesting that both the V and V' sites are occupied by the Mu, regardless of the H/D content. The fact that the observed linewidth in LaScSiD_{1.2} [$\Delta = 0.286(1)$ MHz] is nearly identical to the mean of those estimated for the two sites (0.144 and 0.340 MHz) suggests a similar scenario in LaScSiD_{1.2}. The dispersed H occupancy over both the V and V' sites can be explained by the gain in entropy. Thus, the vacant V sites are made available to the Mu (see the next paragraph). The observed value of Δ_1 is in reasonable agreement with that calculated for the V site, irrespective of the H content; however, Δ_2 is approximately 20% larger than that estimated for the V' site in LaScSiH and LaScSiH_{1.5} (see Table I). In NdScSiD_{1.5}, which has the same crystal structure as LaScSiH_{1.5}, neutron diffraction measurements have indicated that D at the V' site is localized slightly off the c axis from the Sc₄ plane [28]. However, this displacement leads to a decrease in Δ , in contrast to the observed trend. Therefore, we tentatively attribute the discrepancy to the possibility that the local field distribution differs from the Gaussian distribution (a prerequisite of the Kubo-Toyabe function) because of the random occupation of the V' site by H near the Mu. As inferred from the temperature dependence of f_V shown in Fig. 3, the occupancy of the V sites increases with temperature regardless of the H/D content, indicating that the Mu preferentially occupies the V sites at higher temperatures. This is consistent with the general assumption that the initial Mu occupancy is that of a quenched state (corresponding to $T \rightarrow \infty$) determined by the density of the available sites (e.g., $f_V \simeq 2/3$ for $x = 0$). As the temperature increases, f_V is expected to approach the equilibrium distribution [$\simeq 2/(2 + e^{-\Delta\varepsilon/k_B T})$] at $x = 0$, where $\Delta\varepsilon$ is the energy difference between the two sites]. Note that the H occupancy is described by the equilibrium distribution, where H exhibits a smaller V site occupancy at higher temperatures.

Considering that the Mu is a microscopic entity for probing the local motion averaged over a time range limited by the muon lifetime (approximately $10^1 \mu\text{s}$), we assume that the temperature dependence of f_V is determined by the migration of the muons from the V' to V sites via hopping motion, which

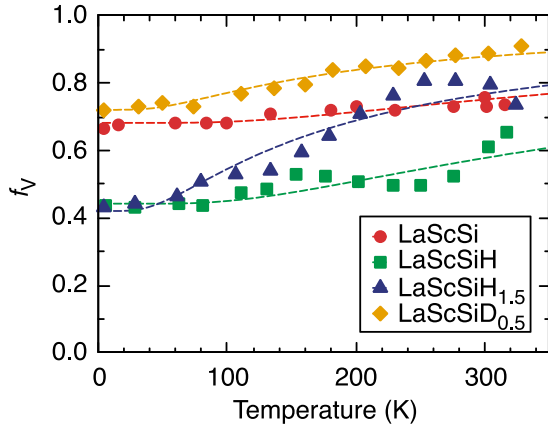


FIG. 3. Temperature dependence of fractional yields for muons localized at the V site determined by $f_V \equiv A_1/(A_1 + A_2)$. The errors are smaller than the symbol size. The dashed curves are the best fits of Eq. (2).

is controlled by a potential barrier ε (not $\Delta\varepsilon$),

$$f_V(T) = f_V^0 + (1 - f_V^0)e^{-\varepsilon/k_B T}, \quad (2)$$

where f_V^0 is the initial Mu occupancy of the V sites (see Supplemental Material [25]). The dashed curves in Fig. 3 are fitted with the aforementioned model. The temperature dependence is reasonably reproduced except for LaScSiH in which A_c is significantly enhanced at high temperatures. The deduced parameter values are $f_V^0 = 0.682(5)$, $0.44(2)$, $0.41(3)$, and $0.721(9)$, and $\varepsilon = 39(3)$, $37(4)$, $13(1)$, and $15(1)$ meV for LaScSi, LaScSiH, LaScSiD_{0.5}, and LaScSiH_{1.5}, respectively. These results are consistent with the assumption that the Mu localizes at the V site as the true ground state at higher temperatures; this is also in line with the stepwise hydrogenation process proposed in the literature [13]. Bader charge analysis [29] of H localized at the V and V' site centers in the dilute limit results in $H^{-0.63}$ and $H^{-0.80}$, respectively, suggesting that the corresponding Mu charge state is Mu^- .

B. Anomalous diamagnetism of electride electrons

In the high transverse field (HTF)- μ SR measurement, the curve-fit analysis is conducted using the equation

$$A(t) = A_\alpha \exp\left(-\frac{\Delta^2 t^2}{2}\right) \cos(\omega t + \phi_\alpha), \quad (3)$$

where A_α ($\alpha = \pm\hat{x}, \pm\hat{y}$) is the asymmetry at $t = 0$, and ϕ_α is the initial phase of the spin rotation. We note that the V and V' sites are not discernible by the frequency shift [as inferred from the fast Fourier transform (FFT) of the HTF- μ SR spectra shown in the Supplemental Material [25], Fig. S3]. Therefore, we adapt a single-component analysis in which the shift K_μ is evaluated from the angular frequency ω as follows:

$$K_\mu = \frac{\omega - \gamma_\mu B_{\text{ref}}}{\gamma_\mu B_{\text{ref}}} - K_D, \quad (4)$$

$$K_D = (4\pi/3 - N_z)\chi, \quad (5)$$

where $\gamma_\mu/2\pi = 135.53$ (MHz/T) is the muon gyromagnetic ratio; K_D (expressed in cgs units) is the correction term for the

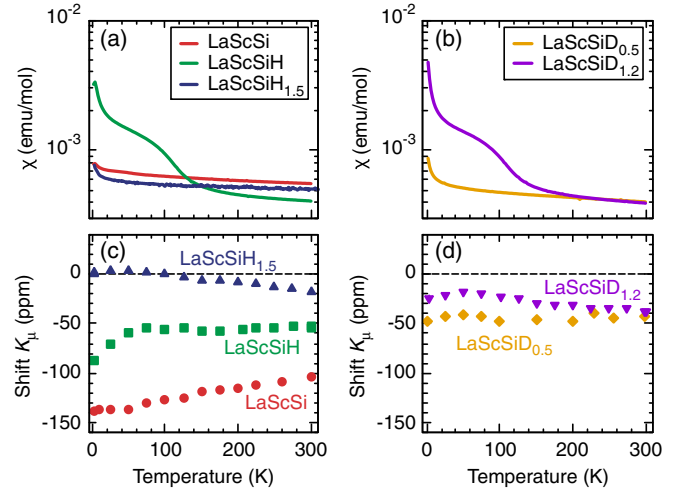


FIG. 4. Temperature dependence of the (a),(b) uniform magnetic susceptibility, χ , and (c),(d) μ SR frequency shift, K_μ , in LaScSiH/D_x. The error bars are smaller than the symbol size.

Lorentz and demagnetization fields; N_z is the demagnetization factor, which depends on the geometry of the sample [30]; and χ is the uniform susceptibility. The reference field B_{ref} is simultaneously monitored through the precession frequency of the muons stopped in a scintillator slab made of a nonmagnetic insulator CaCO_3 , placed immediately behind the sample. This scintillator serves as a muon “veto” counter so that the muons stopped in the sample and those stopped in the scintillator slab can be recorded separately. The instrument-specific temperature drift in B_{ref} is calibrated through additional measurements on a silver sample.

The temperature dependence of χ and K_μ for LaScSi and its hydrides/deuterides is shown in Fig. 4. It is noticeable that χ exhibits a significant increase below approximately 150 K in LaScSiH and LaScSiD_{1,2}, which is probably due to the unknown impurity phase(s). In other samples, χ exhibits mostly temperature-independent (Pauli paramagnetismlike) behavior. The magnitude of χ above approximately 150 K is the largest in pristine LaScSi, and this is in agreement with the results reported in the literature [13]. This is also consistent with the results of the DFT calculations, where the density of states near E_F is the largest in LaScSi. We note that the demagnetization correction (K_D) may be inaccurate at lower temperatures for LaScSiH and LaScSiD_{1,2} because the relative uncertainty associated with N_z is increased by the larger χ below approximately 150 K. We can assume that K_μ is negative and mostly independent of temperature. In particular, K_μ in LaScSi is as large as -150 ppm. This cannot be easily explained by the conventional chemical shifts as observed in C12A7 [31].

The magnitude of K_μ in hydrogenated LaScSi exhibits a general decreasing trend with increasing H content. The apparently weaker dependence on x in the deuterated samples may be attributed to the uncertainty in x (see Sec. II). As H is mostly in hydride ions at the V/V' sites, the reduction in K_μ is uniquely ascribed to the decrease in the number of electride electrons due to their partial adsorption into H. This trend also suggests that the rest of the electride electrons remain

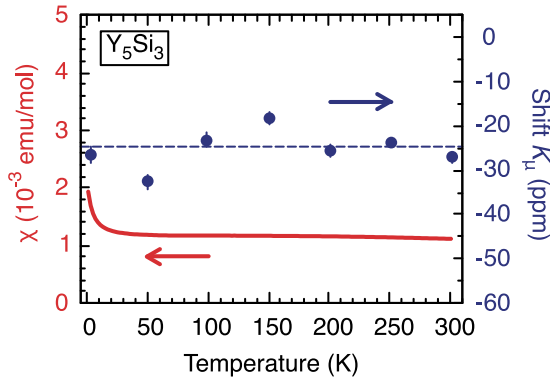


FIG. 5. Temperature dependence of the uniform magnetic susceptibility, χ (left axis), and μ SR frequency shift, K_μ (right axis), in Y_5Si_3 . The dashed line represents the average value over temperature.

delocalized while H intake occurs; K_μ will be unchanged if the Mu probes nearby localized electrons.

Figure 5 shows the temperature dependence of χ and K_μ in Y_5Si_3 . Except for the small Curie term at temperatures below approximately 20 K, χ is almost independent of temperature, indicating that the apparent Pauli paramagnetic contribution dominates. K_μ also exhibits an almost temperature-independent negative shift of approximately -25 ppm, which is qualitatively similar to that in $LaScSiH_x$. (The FFT spectra are shown in the Supplemental Material [25], Fig. S3.)

The results for K_μ in $LaScSiH/D_x$ and Y_5Si_3 , together with the large negative shifts previously observed in single crystalline Y_2C [18], provide compelling evidence that the anomalous diamagnetism inferred from μ SR in these compounds is an important hallmark of electrider electrons in intermetallic compounds involving transition metals.

IV. DISCUSSION

In general, the uniform susceptibility of transition metal compounds is the sum of contributions from various sources,

$$\chi = \chi_{\text{dia}} + \chi_s + \chi_d + \chi_{\text{vv}}, \quad (6)$$

where χ_{dia} is the diamagnetism of conduction electrons, χ_s (χ_d) is the spin susceptibility of s (d) band electrons, and χ_{vv} is the Van Vleck orbital susceptibility. The corresponding muon Knight shift is then expressed as

$$K_\mu = K_{\text{dia}} + K_s + K_d + K_{\text{vv}}. \quad (7)$$

The sum of χ_s (Pauli paramagnetism) and χ_{dia} ($= -\chi_s/3$ for Landau diamagnetism) gives a positive and small contribution to K_μ in simple metals, whereas the contributions of d electrons can be large, with its signs determined by the hyperfine field (H_{hf}). In conventional metals, relatively large diamagnetic shifts have been observed by μ SR only in metals with strong s - d hybridization, such as Ni, Pd, and Pt, in which the

contribution of d electrons has been inferred from the Curie-Weiss behavior of χ_d and K_d [32–36]. In $LaScSi$ and Y_5Si_3 (as in Y_2C), strong hybridization of the electrider electron and rare-earth atoms has been reported [13,14,21]. However, the absence of the Curie-Weiss behavior in K_μ suggests that no such contribution exists in the electrideres.

One possible origin of the temperature-independent diamagnetism is the Van Vleck term associated with the electrider electrons,

$$\chi_{\text{vv}} = 2N \sum_i \frac{|(i|J_z|0)|^2}{E_i - E_0}, \quad (8)$$

where N is the density of atoms per unit lattice, J_z is the angular momentum operator, $|i\rangle$ is the excited state that has a finite orbital angular momentum, $|0\rangle$ is the ground state, and E_i and E_0 are their respective eigenenergies. Here, the contribution of the d orbitals is expected to be larger owing to the strong s - d hybridization with the electrider electrons. Because $E_i - E_0$ is generally sufficiently larger than $k_B T$, χ_{vv} does not vary with temperature. The negative sign of K_μ can be reasonably attributed to the magnetic dipole character of H_{hf} between the Mu and the off-site d electrons, where the shift is given by the following relation: $K_\mu = H_{\text{hf}} \chi_{\text{vv}}$.

Another possibility is an anomaly in the Landau diamagnetism due to the Dirac electronlike dispersion relation [37]. The DFT calculations for these electrideres suggest a slight deviation from the quadratic dispersion relation for the electrider bands near the Fermi level, which may lead to an enhanced χ_{dia} (not exceeding Pauli paramagnetism) and K_{dia} [38].

A closer look at Figs. 4(c) and 4(d) shows that K_μ exhibits a slight decrease with increasing temperature in $LaScSi$. As x increases, K_μ at 300 K approaches zero. The temperature-dependent trend in $LaScSiH_{1.5}$ is opposite that in $LaScSi$. This trend can be explained by the temperature variation of f_V , which leads to a change in $|K_\mu|$ as the average of the different K_μ values at the V and V' sites.

Finally, the absence of such a large diamagnetism in the prototype electrider, $C12A7 : e^-$, is probably due to the absence of overlaps with other orbitals [4,31]. The relatively small occupancy of the electrider electron sites (1/3 or less) and the associated small density near the Mu may also contribute to the negligible diamagnetism.

ACKNOWLEDGMENTS

We would like to thank the TRIUMF staff for their technical support during the μ SR experiment and N. Hamada for stimulating discussion. This work was supported by the MEXT Elements Strategy Initiative to Form Core Research Center for Electron Materials (Grant No. JPMXP0112101001) and JSPS KAKENHI (Grants No. 19K15033 and No. 17H06153). The μ SR experiments were conducted under user programs (Proposal No. 2013MS01) at the Materials and Life Science Experimental Facility of the J-PARC and M1437 at TRIUMF. The magnetic susceptibility measurements were performed using the instrument at the Neutron Science and Technology Center, CROSS.

- [1] J. L. Dye, *Science* **301**, 607 (2003).
- [2] H. Hosono and M. Kitano, *Chem. Rev.* **121**, 3121 (2021).
- [3] S. Matsuishi, Y. Toda, M. Miyakawa, K. Hayashi, T. Kamiya, M. Hirano, I. Tanaka, and H. Hosono, *Science* **301**, 626 (2003).
- [4] S. Matsuishi, S. W. Kim, T. Kamiya, M. Hirano, and H. Hosono, *J. Phys. Chem. C* **112**, 4753 (2008).
- [5] Y. Toda, H. Yanagi, E. Ikenaga, J. Kim, M. Kobata, S. Ueda, T. Kamiya, M. Hirano, K. Kobayashi, and H. Hosono, *Adv. Mater.* **19**, 3564 (2007).
- [6] M. Kitano, Y. Inoue, Y. Yamazaki, F. Hayashi, S. Kanbara, S. Matsuishi, T. Yokoyama, S.-W. Kim, M. Hara, and H. Hosono, *Nat. Chem.* **4**, 934 (2012).
- [7] M. Kitano, S. Kanbara, Y. Inoue, N. Kuganathan, P. V. Sushko, T. Yokoyama, M. Hara, and H. Hosono, *Nat. Commun.* **6**, 6731 (2015).
- [8] K.-B. Kim, M. Kikuchi, M. Miyakawa, H. Yanagi, T. Kamiya, M. Hirano, and H. Hosono, *J. Phys. Chem. C* **111**, 8403 (2007).
- [9] H. Buchammagari, Y. Toda, M. Hirano, H. Hosono, D. Takeuchi, and K. Osakada, *Org. Lett.* **9**, 4287 (2007).
- [10] M. Ruzsak, M. Inger, S. Witkowski, M. Wilk, A. Kotarba, and Z. Sojka, *Catal. Lett.* **126**, 72 (2008).
- [11] Y. Adachi, S.-W. Kim, T. Kamiya, and H. Hosono, *Mater. Sci. Eng. B* **161**, 76 (2009).
- [12] Y. Toda, H. Hirayama, N. Kuganathan, A. Torrisi, P. V. Sushko, and H. Hosono, *Nat. Commun.* **4**, 2378 (2013).
- [13] J. Wu, Y. Gong, T. Inoshita, D. C. Fredrickson, J. Wang, Y. Lu, M. Kitano, and H. Hosono, *Adv. Mater.* **29**, 1700924 (2017).
- [14] Y. Lu, J. Li, T. Tada, Y. Toda, S. Ueda, T. Yokoyama, M. Kitano, and H. Hosono, *J. Am. Chem. Soc.* **138**, 3970 (2016).
- [15] B. Chevalier, W. Hermes, B. Heying, U. C. Rodewald, A. Hammerschmidt, S. F. Matar, E. Gaudin, and R. Pöttgen, *Chem. Mater.* **22**, 5013 (2010).
- [16] I. McColm, V. Kotrocvco, T. Button, N. Clark, and B. Bruer, *J. Less-Common Met.* **115**, 113 (1986).
- [17] K. Hayashi, S. Matsuishi, T. Kamiya, M. Hirano, and H. Hosono, *Nature (London)* **419**, 462 (2002).
- [18] M. Hiraishi, K. M. Kojima, I. Yamauchi, H. Okabe, S. Takeshita, A. Koda, R. Kadono, X. Zhang, S. Matsuishi, H. Hosono, K. Hirata, S. Otani, and N. Ohashi, *Phys. Rev. B* **98**, 041104(R) (2018).
- [19] L. Liu, C. Wang, S. Yi, D. K. Kim, C. H. Park, and J.-H. Cho, *Phys. Rev. B* **99**, 220401(R) (2019).
- [20] T. Inoshita, S. Jeong, N. Hamada, and H. Hosono, *Phys. Rev. X* **4**, 031023 (2014).
- [21] X. Zhang, Z. Xiao, H. Lei, Y. Toda, S. Matsuishi, T. Kamiya, S. Ueda, and H. Hosono, *Chem. Mater.* **26**, 6638 (2014).
- [22] H. Tamatsukuri, Y. Murakami, Y. Kuramoto, H. Sagayama, M. Matsuura, Y. Kawakita, S. Matsuishi, Y. Washio, T. Inoshita, N. Hamada, and H. Hosono, *Phys. Rev. B* **102**, 224406 (2020).
- [23] H. Okabe, M. Hiraishi, S. Takeshita, A. Koda, K. M. Kojima, and R. Kadono, *Phys. Rev. B* **98**, 075210 (2018).
- [24] K. M. Kojima, M. Hiraishi, H. Okabe, A. Koda, R. Kadono, K. Ide, S. Matsuishi, H. Kumomi, T. Kamiya, and H. Hosono, *Appl. Phys. Lett.* **115**, 122104 (2019).
- [25] See Supplemental Material at <http://link.aps.org/supplemental/10.1103/PhysRevB.103.L241101> for details on the experiments and DFT, temperature dependence of f_V , and FFT spectra in HTF- μ SR.
- [26] R. S. Hayano, Y. J. Uemura, J. Imazato, N. Nishida, T. Yamazaki, and R. Kubo, *Phys. Rev. B* **20**, 850 (1979).
- [27] R. Kadono, K. Shimomura, K. H. Satoh, S. Takeshita, A. Koda, K. Nishiyama, E. Akiba, R. M. Ayabe, M. Kuba, and C. M. Jensen, *Phys. Rev. Lett.* **100**, 026401 (2008).
- [28] S. Tencé, T. Mahon, E. Gaudin, B. Chevalier, J.-L. Bobet, R. Flacau, B. Heying, U. C. Rodewald, and R. Pöttgen, *J. Solid State Chem.* **242**, 168 (2016).
- [29] W. Tang, E. Sanville, and G. Henkelman, *J. Phys.: Condens. Matter* **21**, 084204 (2009).
- [30] M. Sato and Y. Ishii, *J. Appl. Phys.* **66**, 983 (1989).
- [31] M. Hiraishi, K. M. Kojima, M. Miyazaki, I. Yamauchi, H. Okabe, A. Koda, R. Kadono, S. Matsuishi, and H. Hosono, *Phys. Rev. B* **93**, 121201(R) (2016).
- [32] A. Schenck, *Muon Spin Rotation Spectroscopy: Principles and Applications in Solid State Physics* (Adam Hilger, Bristol, 1985).
- [33] J. A. Seitchik, A. C. Gossard, and V. Jaccarino, *Phys. Rev.* **136**, A1119 (1964).
- [34] P. J. Segransan, Y. Chabre, and W. G. Clark, *J. Phys. F: Met. Phys.* **8**, 1513 (1978).
- [35] F. Gygax, W. Rüegg, A. Schenck, H. Schilling, W. Studer, and R. Schulze, *J. Magn. Magn. Mater.* **15-18**, 1191 (1980).
- [36] F. N. Gygax, A. Hintermann, W. Rüegg, A. Schenck, W. Studer, A. J. van der Wal, and L. Schlapbach, *Hyperfine Interact.* **15**, 533 (1983).
- [37] Y. Fuseya, M. Ogata, and H. Fukuyama, *J. Phys. Soc. Jpn.* **84**, 012001 (2015).
- [38] N. Hamada (private communication).